V2V Communication Systems under Correlated Double-Rayleigh Fading Channels

Petros S. Bithas, Konstantinos Maliatsos and Athanasios G. Kanatas
Department of Digital Systems, University of Piraeus, Greece e-mail: {pbithas;kmaliat;kanatas}@unipi.gr

***Abstract*—In this paper, the correlated double-Rayleigh distribution is introduced and analyzed. This distribution has been found to provide an accurate statistical description of the vehicle-to-vehicle multipath propagation. Novel infinite series expressions for the joint probability density and the cumulative distribution functions are derived, while the joint moments are also obtained in closed form. Although the new statistical metrics can be employed in a wide range of applications, this paper focuses on the performance of dual-branch selection diversity receivers. In this context, the outage probability (OP) and the average bit error rate (ABER) of dual-branch selection diversity operating over double-Rayleigh fading channels are analytically evaluated. Moreover, an asymptotic analysis is also included, resulting to simpler closed-form expressions for the OP and ABER. Finally, the applicability of the analytical results were verified using the measurements based WINNER2 models.**

***Index Terms*- Bit error rate, correlated double-Rayleigh, outage probability, selection diversity, vehicle-to-vehicle communications.**

I. Introduction

The vehicle-to-vehicle (V2V) communication systems have recently attracted the interest of the scientific community and the industry, since they can directly be applied to intelligent transportation systems (ITS). As a result, clear benefits are offered, including road safety, traffic efficiency and comfort to both drivers and passengers [1]. An important factor that is directly related with these systems performance is the channel model. In general, the channel model of these systems is sufficiently different from the classical cellular channel [2]. Reasons for this include, the equal heights of the transmitter (Tx) and the receiver (Rx), their movement, the surrounding scatterers, the highly dynamic propagation conditions etc. Since multipath channels can efficiently be described by using proper statistical models, the performance of these systems can be studied by selecting an appropriate distribution. A well established channel distribution that has been widely used to model non line-of-sight (NLoS) V2V channel conditions is the double-Rayleigh process, e.g., [3]–[5], which represents a special case of the multiple scattering radio channel. Based on the multiple scattering modeling, several studies have analyzed the performance of inter-vehicular communication systems that support diversity reception [6]–[8].

Regardless of the channel model that has been adopted, an important factor that seriously affects the system performance is the existence of correlation among the diversity branches. In general, such signal correlation exists in cases where the distance between the diversity antennas is small. The open research literature concerning correlated distributions is quite extensive, e.g., [9], [10]. In addition, depending upon the antenna placement in the vehicle, e.g., at the mirror or the signs, it will not be surprising that correlation effects will also be present in V2V communication scenarios. However, to the best of the authors' knowledge, bivariate double-Rayleigh distribution and the performance of multi-antenna V2V communication systems over such channels is not available in the open technical literature and thus is the subject of the current work.

Motivated by this important limitation, in this paper, we study for the first time the influence of the correlation effects in a V2V communication scenario. To this aim, we first introduce the bivariate double-Rayleigh distribution. In particular, we present novel expressions for important statistical properties of the new distribution, such as the joint probability density function (PDF) and cumulative distribution function (CDF) as well as the joint moments. The new distribution can be applied to different research fields. However, in this work, we focus on a diversity reception scenario. More specifically, we investigate the performance of a dual-branch selection diversity (SD) operating in a bivariate double-Rayleigh fading channels environment.

The rest of the paper is organized as follows. Section II contains important statistical metrics of the bivariate double-Rayleigh distribution. In Section III, the performance analysis of a SD Rx is performed in terms of the outage probability (OP), average bit error rate (ABER), while an asymptotic analysis is also included. Section IV presents some numerical results and Section V includes concluding remarks.

II. Correlated Double-Rayleigh Statistics

Let $X_i, (i = 1, 2, 3)$ denoting the envelopes of zero mean complex Gaussian random variables (RV)s with marginal PDF given by [11, eq. (2.6)]

$$f_{X_i}(x) = \frac{2x}{\Omega_i} \exp\left(-\frac{x^2}{\Omega_i}\right) \tag{1}$$

where Ω_i is the mean square value. Moreover, the double-Rayleigh RV is a product of two independent Rayleigh RVs [3]. In this context, let Z_j, with $j = 1, 2$, be defined as

$$\begin{aligned} Z_1 &= X_1 \times X_2 \\ Z_2 &= X_1 \times X_3. \end{aligned} \tag{2}$$

This paper is based on the fact that X_2 and X_3 are correlated Rayleigh RVs with joint PDF given by [11, eq. (6.2)]

$$\begin{aligned} f_{X_2,X_3}(x,y) = &\frac{4xy}{\Omega_2\Omega_3(1-\rho)} \exp\left[-\frac{1}{1-\rho}\left(\frac{x^2}{\Omega_2}+\frac{y^2}{\Omega_3}\right)\right] \\ &\times I_0\left[\frac{2\sqrt{\rho}xy}{(1-\rho)\sqrt{\Omega_2\Omega_3}}\right] \end{aligned} \tag{3}$$

where $I_v(\cdot)$ is the modified Bessel function of the first kind and order v [12, eq. (8.406/1)] and $\rho = \mathrm{cov}\left(X_2^2, X_3^2\right)/\sqrt{\mathrm{var}\left(X_2^2\right)\mathrm{var}\left(X_3^2\right)}$ is the power correlation coefficient $(0 \leq \rho < 1)$ [11]. Since Z_1 and Z_2 constitute products of two RVs, their joint PDF is given by

$$f_{Z_1,Z_2}(z,w) = \int_0^\infty \frac{1}{x_1^2} f_{X_1}(x_1) f_{X_2,X_3}\left(\frac{z}{x_1}, \frac{w}{x_1}\right) dx_1. \quad (4)$$

Substituting (1) and (3) in (4), employing the infinite series representation of the Bessel function, [12, eq. (8.445)], making a change of variables and using [12, eq. (3.471/9)] yields the following expressions for the joint PDF of Z_1 and Z_2

$$f_{Z_1,Z_2}(z,w) = \frac{1/2}{\Omega_1\sqrt{\rho\Omega_2\Omega_3}} \sum_{k=0}^{\infty} \left(\frac{1-\rho}{z^2/\Omega_2 + w^2/\Omega_3}\right)^{k+\frac{1}{2}} \times \frac{1}{(k!)^2}\left(\frac{zw\sqrt{\rho}/4}{\sqrt{\Omega_1\Omega_2\Omega_3}(1-\rho)^2}\right)^{2k+1} K_{2k+1}\left(\frac{\sqrt{\frac{z^2}{\Omega_2}+\frac{w^2}{\Omega_3}}}{2\sqrt{(1-\rho)\Omega_1}}\right) \quad (5)$$

where $K_v(\cdot)$ is the modified Bessel function of the second kind and order v [12, eq. (8.432/1)].

Assuming identical mean square values, i.e., $\Omega_i = \Omega$, the joint CDF of Z_1, Z_2 is given in (6) (shown at the top of the next page). In (6),

$$\mathcal{F}_1(x) = \frac{(2k-p)!}{p!\xi^{2p-2k-1}} \frac{(-1)^p}{\Gamma(2k+1-p)} \mathcal{G}_{3,3}^{2,2}\left(x\middle|\begin{matrix}1-(p-k),1,k+2\\ 1+2k-p,1+k,k-p\end{matrix}\right)$$

$$\mathcal{F}_2(x) = \frac{1}{2(p+k-m+1)} \mathcal{G}_{2,2}^{1,2}\left(x\middle|\begin{matrix}0,m-p-k-1\\ 0,-(p+k-m+2)\end{matrix}\right)$$

$$\mathcal{F}_3(x) = \frac{1}{2}\mathcal{G}_{3,3}^{2,2}\left(x\middle|\begin{matrix}1,1-(p+k-m),k+m+3\\ 1,k+m+2,m-p-k\end{matrix}\right).$$

Moreover, $\xi = \sqrt{1-\rho}\Omega$, $\mathcal{G}_{p,q}^{m,n}[\cdot|\cdot]$ denotes the Meijer's G-function [12, eq. (9.301)], ${}_2F_1(\cdot)$ is the Gauss hypergeometric function [12, eq. (9.100)], $\Gamma(\cdot)$ is the Gamma function [12, eq. (8.310/1)] and $\psi(\cdot)$ is the Euler's psi function [12, eq. (8.360/1)]. The proof of (6) is given in the Appendix.

In addition, using (5) in the definition of the joint moments $\mu(n_1,n_2) = \mathbb{E}\left\langle Z_1^{n_1} Z_2^{n_2}\right\rangle$, where $\mathbb{E} < \cdot >$ denotes expectation, making a change of variables of the form $x = y^2$, using first [13, eq. (2.16.3/8)], then [12, eq. (6.561/16)] as well as the definition of the Gauss hypergeometric function, yields the following closed-form expression for the joint moments

$$\mu(n_1,n_2) = \Omega^{n_1+n_2}(1-\rho)^{\frac{n_1+n_2}{2}+1}\Gamma\left(\frac{n_1+n_2}{2}+1\right) \times \Gamma\left(1+\frac{n_1}{2}\right)\Gamma\left(1+\frac{n_2}{2}\right){}_2F_1\left(\frac{n_1}{2}+1, \frac{n_2}{2}+1, 1, \rho\right). \quad (7)$$

It should be noted that to the best of the authors knowledge, all the previously derived expressions for the correlated double-Rayleigh distribution have not been reported in the past.

III. SD Receivers Performance

In principle, the previous derived expressions can be used in various research scenarios, where bivariate double-Rayleigh statistics is necessary. However, the research is focused on diversity reception scenario. Thus, let us consider a single input multiple output (SIMO) communication system, supporting SD Rx, operating over flat fading, which is modeled by the previously discussed distribution.

The instantaneous signal-to-noise (SNR) at the ith branch, with $i = 1, 2$, is defined as

$$\gamma_i = Z_i^2 \frac{E_s}{N_0} \quad (8)$$

with E_s denoting the transmitted symbol energy and N_0 the power spectral density of the additive white Gaussian noise (AWGN) channel. The corresponding average SNR is given by $\overline{\gamma}_i = \mathbb{E}\left\langle Z_i^2\right\rangle E_s/N_0$. Additionally, since the instantaneous SNR at the output of the SD Rx is $\gamma_{\mathrm{sd}} = \max\{\gamma_1, \gamma_2\}$, its CDF can be expressed as $F_{\gamma_{\mathrm{sd}}}(\gamma) = F_{\gamma_1,\gamma_2}(\gamma,\gamma)$. Using (6), assuming $\overline{\gamma}_i = \overline{\gamma}$ and based on the information provided above, it is not difficult to recognize that the CDF of γ_{sd} is given by

$$F_{\gamma_{\mathrm{sd}}}(\gamma) = \frac{2}{\overline{\gamma}^3}\sum_{k=0}^{\infty}\frac{1}{(k!)^2}\left(\frac{\rho}{\overline{\gamma}^2}\right)^k\left(\frac{1}{1-\rho}\right)^{k+\frac{1}{2}} \times \left\{\frac{1}{2}\sum_{\substack{p=0\\ p\neq k}}^{2k}\mathcal{F}_1(1)\frac{\gamma^{p+1}}{\Gamma(2k+1-p)} + \mathcal{F}_4\gamma^{k+1} + (-1)^{2k+2} \times \left[\sum_{p=0}^{\infty}\frac{(1/\xi)^{2p+2k+1}}{p!(2k+p+1)!}\gamma^{2(1+k)+p}\left[\sum_{m=0}^{p}\frac{\binom{p}{m}}{k+m+1} \times \left[\left[\frac{\ln\left(\sqrt{2\gamma}/\xi\right)}{p+k-m+1} - \mathcal{F}_2(1)\right] - \mathcal{F}_3(1)\right] - \mathcal{F}_5\right]\right]\right\} \quad (9)$$

where

$$\mathcal{F}_4 = \frac{(-1)^{k+1}\xi}{k+1}\left(\sum_{t=2}^{k+1}\frac{{}_2F_1\left(k+1, k+2-t; k+2; -1\right)}{k+2-t} - \left(\left(1-(-1)^{k+1}\right)\ln(2) + \sum_{t=1}^{k+1}\frac{(-1)^t}{(k-t+2)} + \frac{1}{k+1}\right)\right)$$

$$\mathcal{F}_5 = \frac{1}{2}\sum_{m=0}^{p}\frac{\binom{p}{m}}{k+p-m+1}\frac{\psi(p+1)+\psi(2k+p+2)}{k+m+1}.$$

Next, based on the analytical expression for the CDF of the output SNR, the performance will be investigated using the OP and the ABER.

A. Outage Probability

OP is defined as the probability that the SNR falls below a predetermined threshold γ_{th} and is given by $P_{\mathrm{out}} = F_{\gamma_{\mathrm{sd}}}(\gamma_{\mathrm{th}})$. *Asymptotic Analysis:* In order to clearly understand important system-design parameters, we study the asymptotic OP. This approach help us to quantify the amount of performance variations, which are due to the fading effects as well as to the Rx's architecture. For higher mean square values of Ω_i, the PDF of X_i can be closely approximated by $f_{X_i}(x) \approx \frac{2x}{\Omega_i}$. Based on this approximated expression, and by following a

$$F_{Z_1,Z_2}(z,w)=\frac{2}{\Omega^3}\sum_{k=0}^{\infty}\frac{1}{(k!)^2}\left(\frac{\rho}{\Omega^2}\right)^k\left(\frac{1}{1-\rho}\right)^{k+\frac{1}{2}}\left\{\frac{1}{2}\sum_{\substack{p=0\\p\neq k}}^{2k}\mathcal{F}_1\left(\frac{w^2}{z^2}\right)z^{2(k+1)}w^{2(p-k)}+(-1)^k\xi w^{2(1+k)}\left(\frac{(-1)}{k+1}\right.\right.$$
$$\left(\sum_{t=2}^{k+1}\frac{1}{k+2-t}{}_2F_1\left(k+1,k+2-t;k+2;-\frac{w^2}{z^2}\right)-\left(\ln(z^2)+\left(1-\frac{(-z^2)^{k+1}}{w^{2(k+1)}}\right)\ln\left(1+\frac{w^2}{z^2}\right)+\sum_{t=1}^{k+1}\frac{(-1)^t}{k-t+2}\left(\frac{z^2}{w^2}\right)^{t-1}\right.\right.$$
$$\left.\left.\left.-\frac{(1+k)\ln\left(w^2\right)-1}{k+1}\right)\right)\right)+(-1)^{2k+2}\left[\sum_{p=0}^{\infty}\frac{(1/\xi)^{2p+2k+1}}{p!(2k+p+1)!}\left[\sum_{m=0}^{p}\binom{p}{m}\frac{z^{2(k+m+1)}}{w^{2(m-k-p)}}\left[\frac{w^2}{k+m+1}\left[\frac{\ln\left(\sqrt{z^2+w^2}/\xi\right)}{p+k-m+1}-\frac{w^2}{z^2}\mathcal{F}_2\left(\frac{w^2}{z^2}\right)\right]\right.\right.\right.$$
$$\left.\left.\left.-\frac{z^2/2}{k+m+1}\mathcal{F}_3\left(\frac{w^2}{z^2}\right)\right]\right.\right.\left.\left.-\frac{1}{2}\psi(p+1)\sum_{m=0}^{p}\binom{p}{m}\frac{z^{2(k+m+1)}}{k+m+1}\frac{w^{2(k+p-m+1)}}{k+p-m+1}-\frac{1}{2}\psi(2k+p+2)\sum_{m=0}^{p}\binom{p}{m}\frac{z^{2(k+m+1)}}{k+m+1}\frac{w^{2(k+p-m+1)}}{k+p-m+1}\right]\right]\right\}. \tag{6}$$

similar procedure as the one presented in the Appendix, the CDF of $\gamma_{\rm sd}$ simplifies to the following expression

$$F_{\gamma_{\rm sd}}(\gamma)\approx\frac{\gamma}{\overline{\gamma}^2}\left[\sum_{k=1}^{\infty}\frac{\rho^k}{(k!)^2}\frac{\Gamma(2k+1)}{k+1}\left(\frac{\Gamma(k+2)\Gamma(k)}{\Gamma(2k+1)}\right.\right.$$
$$\left.\left.-\frac{{}_pF_q(2k+1,k+1,k;k+2,k+1;-1)}{k}\right)+2\ln(2)\right] \tag{10}$$

where ${}_pF_q(\cdot)$ is the generalized hypergeometric function [12, eq. (9.14/1)]. Moreover, by employing [14, eqs. (07.23.17.0056.01 and 07.23.03.0025.01)], after some mathematical simplifications and using [14, eq. (01.04.02.0001.01)], yields the following closed-form expression

$$F_{\gamma_{\rm sd}}(\gamma)\approx\frac{2\gamma}{\overline{\gamma}^2}\left[\ln(2)+\ln\left(\frac{1+\sqrt{1-\rho}}{2}\right)-\frac{\ln(1-\rho)}{2}\right]. \tag{11}$$

From (11), it is obvious that ρ will not affect the diversity order, which is always 2, but only the coding gain.

B. Average Bit Error Probability

Using the CDF-based approach the ABER is given by [15]

$$P_{\rm b}=\int_0^{\infty}-P_e'(\gamma)\,F_{\gamma_{\rm sd}}(\gamma)d\gamma \tag{12}$$

where $-P_e'(\gamma)$ denotes the negative derivative of the conditional error probability. For example, assuming differential binary phase shift keying (DBPSK) modulation, $-P_e'(\gamma)=\alpha\beta\exp(-\beta\gamma)$, where $\alpha=1/2,\beta=1$ [15]. Substituting (9) in (12), employing [13, eq. (2.6.21/2)] and after some mathematical manipulations yields

$$P_b=\frac{2}{\overline{\gamma}^3}\sum_{k=0}^{\infty}\frac{1}{(k!)^2}\left(\frac{\rho}{\overline{\gamma}^2}\right)^k\left(\frac{1}{1-\rho}\right)^{k+\frac{1}{2}}\left\{\frac{1}{2}\sum_{\substack{p=0\\p\neq k}}^{2k}\mathcal{F}_1(1)\right.$$
$$\times\frac{\Gamma(p+2)/2}{\Gamma(2k+1-p)}+\mathcal{F}_4\frac{\Gamma(k+2)}{2}+(-1)^{2k+2}\left[\sum_{p=0}^{\infty}\frac{1}{p!}\right.$$
$$\times\frac{(1/\xi)^{2p+2k+1}}{(2k+p+1)!}\frac{\Gamma(2k+p+3)}{2}\left[-\mathcal{F}_3(1)+\sum_{m=0}^{p}\frac{\binom{p}{m}}{k+m+1}\right.$$
$$\left.\left.\left.\times\left[\frac{2\ln(2/\xi)+\psi(2k+p+3)-\ln(2)}{2(p+k-m+1)}-\mathcal{F}_2(1)\right]\right]-\mathcal{F}_5\right]\right\}. \tag{13}$$

Here, it is important to note that the derivation of (13), and thus the investigation of the ABER performance, is only possible by using the analytical approach presented in Section II and the CDF expression given in (9).

Asymptotic Analysis: For the higher mean square values of $\overline{\Omega}_i$, substituting (11) in (12), and after some mathematics, the following convenient closed-form expression for the ABER can be derived

$$P_b\approx\frac{1}{\overline{\gamma}^2}\left[\ln(2)+\ln\left(\frac{1+\sqrt{1-\rho}}{2}\right)-\frac{\ln(1-\rho)}{2}\right]. \tag{14}$$

TABLE I
MINIMUM NUMBER OF TERMS OF (9) REQUIRED FOR OBTAINING ACCURACY BETTER THAN $\pm10^{-5}$.

	$\overline{\gamma}=5dB$		$\overline{\gamma}=15dB$	
γ	$\rho=0.2$	$\rho=0.7$	$\rho=0.2$	$\rho=0.7$
1	3	7	1	5
5	6	8	1	7
10	9	11	2	8

IV. Numerical Results

In this section, various numerical performance evaluation results will be presented. Firstly, the rate of convergence of the infinite series given in (9) has been investigated. More specifically, the minimum number of terms, which guarantees accuracy better than $\pm10^{-5}$ is presented in Table I for different values of γ, ρ and $\overline{\gamma}$. It is clear from these results that only a relatively small number of terms is necessary to achieve an excellent accuracy, while this number is significantly smaller than the corresponding ones for other fading scenarios, e.g., [16]. Moreover, the number of terms increases as γ,ρ increase as well as with the decrease of $\overline{\gamma}$. It is also noted that similar results with Table I were also obtained by using the other infinite series expressions derived in this work, e.g., (13).

In order to evaluate the applicability of the analytical results in real-world conditions, the WINNER2 channel models were used [17]. The objective was to verify that the extracted distributions are representative for SIMO— propagation through keyhole channels using measurement-based models. In keyhole channels, the radio environment in the proximity of both Tx and Rx contains multiple scatterers, while the propagation beyond Tx-Rx proximity and between them is clear with absence of complex propagation phenomena. In order to compose a keyhole with WINNER2, bad urban radio channels (NLoS B2 WINNER) were considered in Tx and Rx

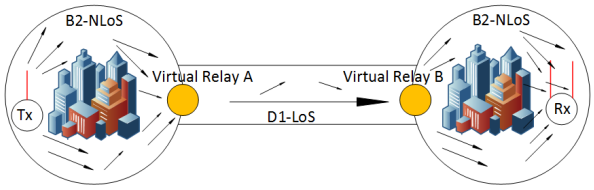

Fig. 1. Keyhole channel as simulated using WINNER2.

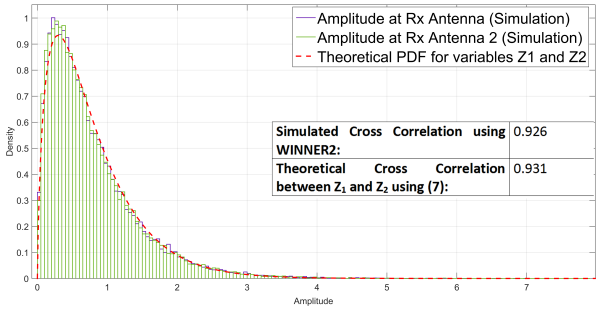

Fig. 2. Histogram using simulation vs. theoretical PDF for Z_1 and Z_2.

proximity, while in-between them rural D1 LoS radio channel was assumed. Moreover, the following assumptions were also made: propagation at 5.9GHz (ITS systems), a single-antenna dipole Tx, two closely spaced dipole antennas for the Rx with interelement distance $\lambda/6$ (λ is the wavelength). Due to strong mutual coupling of the array elements, correlation between the two Rx signals is expected. It is noted that transition between radio environments is not directly supported by WINNER2. Therefore, two virtual relays were considered in the borders of the propagation environments as seen in Fig. 1. The virtual relays are using directional antennas (10^o aperture), since only specific propagation paths in the direction of the Tx-Rx link pass through the keyhole achieving Tx-Rx connectivity.

During simulations, 40,000 WINNER2 narrowband keyhole channels were produced, properly modified to support mobility for both Tx and Rx. Due to the closely spaced elements of the array, the correlation coefficient in the Rx B2 channel was set 0.85. This corresponds to $\rho = (0.85)^2$ as it is defined after (3). In Fig. 2, histograms for the normalized Rx signal amplitude for the two antennas as produced by the WINNER2 vs. the marginal PDF for the keyhole channels as calculated by (5) are presented. It is evident that the modeled channels can be accurately fitted by the theoretical PDF. Moreover, the correlation between the two WINNER2 simulated Tx-Rx channels was calculated and the result was compared with the theoretical one computed by (7). Simulations show that the presented theoretical analysis can be used to successfully characterize keyhole radio channels for SIMO systems.

In Fig. 3, using (9) and assuming $\overline{\gamma} = 9$dB, the OP of dual-branch SD is plotted as a function of the correlation coefficient ρ, for different values of the outage threshold, $\gamma_{\rm th}$. It is depicted that as ρ increases, the performance decreases. This decrease is higher for large values of ρ, i.e., $\rho \geq 0.8$, where the coding gain rapidly minimizes. Moreover, the performance improves with a decrease on $\gamma_{\rm th}$. In the same

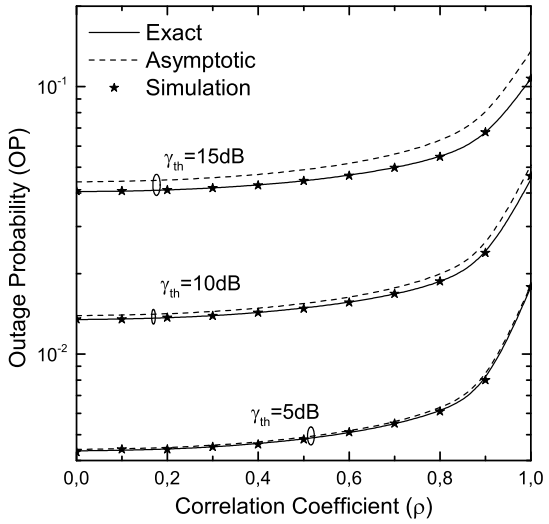

Fig. 3. OP vs ρ, for different values of $\gamma_{\rm th}$.

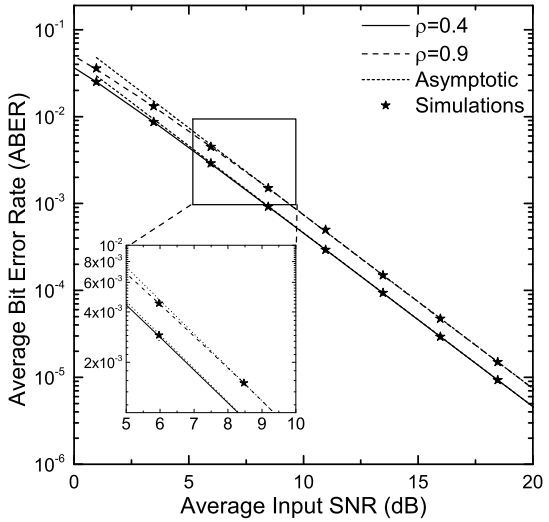

Fig. 4. ABER vs $\overline{\gamma}$, for different values of ρ.

figure, the asymptotic OP, obtained using (11), is also included. It is shown that the difference between the exact and the approximated values decreases with the decrease of $\gamma_{\rm th}$. In Fig. 4, using (13), the ABER is plotted as a function of the average input SNR $\overline{\gamma}$, for different values of the correlation coefficient ρ. Moreover, based on (14), the asymptotic ABER is also included. It is depicted that for lower values of ρ the performance is better. It is important to note that the asymptotic curves approximate quite well the exact ones even for moderate values of the average SNR, i.e., $\overline{\gamma} \geq 10$dB, while this approximation improves for lower values of ρ. Finally, it is noted that the computer simulations performance results, which are also included in all figures, verify in all cases the validity of the proposed theoretical approach.

V. Conclusions

In this paper, the correlated double-Rayleigh distribution is introduced and studied. This model has been widely adopted to describe the V2V multipaths propagation. For this new

distribution, we present novel expressions for important statistical properties, such as the joint PDF, CDF and moments. Although, the new distribution can be applied to different research fields, in this work, we focus on a diversity reception scenario. In particular, we study the performance of a dual-branch SD operating in correlated double-Rayleigh fading channels. It is shown that higher values of the correlation coefficient result to an important reduction to the coding gain and thus the system's performance.

APPENDIX
PROOF FOR EQUATION (6)

Substituting (5) in the definition of the joint CDF, the following integral expressions need to be solved

$$\begin{aligned}\mathcal{I}_1 &= \sum_{p=0}^{2k} \frac{(-1)^p (2k-p)!}{2p!\xi^{2p-2k-1}} \int_0^{z^2}\int_0^{w^2} z^k w^k (z+w)^{p-2k-1} dz dw \\ \mathcal{I}_2 &= \int_0^{z^2}\int_0^{w^2} \frac{\sqrt{z+w}}{\xi} z^k w^k (z+w)^p dz dw \\ \mathcal{I}_3 &= \int_0^{z^2}\int_0^{w^2} z^k w^k (z+w)^p dz dw.\end{aligned} \tag{A-1}$$

In (A-1), $\mathcal{I}_1$ can be rewritten as

$$\begin{aligned}\mathcal{I}_1 =& \sum_{\substack{p=0 \\ p\neq k}}^{2k} \frac{(-1)^p (2k-p)!}{2p!\xi^{2p-2k-1}} \underbrace{\int_0^{z^2}\int_0^{w^2} z^k w^k (z+w)^{p-2k-1} dz dw}_{\mathcal{I}_{1_a}} \\ &+ (-1)^k \xi \underbrace{\int_0^{z^2}\int_0^{w^2} z^k w^k (z+w)^{-k-1} dz dw}_{\mathcal{I}_{1_b}}.\end{aligned} \tag{A-2}$$

By employing [18, eqs. (10 and 28)] as well as using [12, eq. (9.31)], $\mathcal{I}_{1_a}$ can be evaluated as

$$\mathcal{I}_{1_a} = \frac{z^{2(k+1)} w^{2(p-k)}}{\Gamma(2k+1-p)} \mathcal{G}_{3,3}^{2,2}\left(\frac{w^2}{z^2}\middle|\begin{matrix}1+k-p, 1, k+2 \\ 1+2k-p, 1+k, k-p\end{matrix}\right). \tag{A-3}$$

For evaluating $\mathcal{I}_{1_b}$, first we employ [14, eqs. (07.23.16.0001.01 and 07.23.03.0231.01)], then we use [12, eq. (2.729/1)] as well as [13, eq. (1.2.4/3)] and after some mathematical manipulations yields the following expression

$$\begin{aligned}\mathcal{I}_{1_b} =& \frac{(-1) w^{2(k+1)}}{k+1} \left\{ \sum_{t=2}^{k+1} \frac{{}_2F_1\left(k+1, k-t+2; k+2; -\frac{w^2}{z^2}\right)}{k+2-t} \right. \\ &- \left[\ln\left(z^2\right) - \left(1 - \frac{(-z^2)^{k+1}}{w^{2(k+1)}}\right) \ln\left(1+\frac{w^2}{z^2}\right) \right. \\ &\left.\left. + \sum_{t=1}^{k+1} \frac{(-1)^t w^{2(1-t)}}{(k-t+2) z^{2(1-t)}} - \frac{(1+k)\ln(w^2)-1}{1+k} \right] \right\}.\end{aligned} \tag{A-4}$$

For evaluating $\mathcal{I}_2$, we employ the binomial identity and integration by parts, then [18, eqs. (10 and 26)] are used and after a few mathematics yields the following expression

$$\begin{aligned}\mathcal{I}_2 =& \sum_{m=0}^{p} \binom{p}{m} \frac{z^{2(k+m+1)} w^{2(k+p-m)}}{k+m+1} \left\{ \left[\frac{w^2}{k+p-m+1} \right.\right. \\ &\times \left(\ln\left(\frac{\sqrt{z^2+w^2}}{\xi}\right) - \frac{w^2}{2z^2} \mathcal{G}_{2,2}^{1,2}\left(\frac{w^2}{z^2}\middle|\begin{matrix}0, m-p-k-1 \\ 0, m-p-k-2\end{matrix}\right)\right) \Bigg] \\ &\left. - \frac{z^2}{2} \mathcal{G}_{3,3}^{2,2}\left(\frac{w^2}{z^2}\middle|\begin{matrix}1, 1-(p+k-m), k+m+3 \\ 1, k+m+2, m-p-k\end{matrix}\right) \right\}.\end{aligned} \tag{A-5}$$

Finally, the solution of $\mathcal{I}_3$ is given by

$$\mathcal{I}_3 = \sum_{m=0}^{p} \binom{p}{m} \frac{z^{2(k+m+1)}}{k+m+1} \frac{w^{2(k+p-m+1)}}{k+p-m+1}. \tag{A-6}$$

Based on the previous derived analytical expressions and after some analytical manipulations, (6) is finally derived.

ACKNOWLEDGEMENT

This research has received funding from the European Union's Horizon 2020 research and innovation programme under "ROADART" Grant Agreement No 636565.

REFERENCES

[1] G. Rafiq *et al.*, "Whats new in intelligent transportation systems: An overview of European projects and initiatives," *IEEE Vehicular Technology Magazine*, vol. 8, no. 4, pp. 45–69, 2013.

[2] A. F. Molisch, F. Tufvesson, J. Karedal, and C. F. Mecklenbräuker, "A survey on vehicle-to-vehicle propagation channels," *IEEE Wireless Communications*, vol. 16, no. 6, pp. 12–22, 2009.

[3] I. Z. Kovács, P. C. Eggers, K. Olesen, and L. G. Petersen, "Investigations of outdoor-to-indoor mobile-to-mobile radio communication channels," in *IEEE Vehicular Technology Conference*, 2002, pp. 430–434.

[4] J. Salo, H. M. El-Sallabi, and P. Vainikainen, "Impact of double-Rayleigh fading on system performance," in *Proc. 1st IEEE Int. Symp. on Wireless Pervasive Computing, ISWPC 2006*, 2006.

[5] M. Pätzold, B. O. Hogstad, and N. Youssef, "Modeling, analysis, and simulation of MIMO mobile-to-mobile fading channels," *IEEE Trans. Wireless Commun.*, vol. 7, no. 2, pp. 510–520, Feb. 2008.

[6] A. Chelli, R. Hamdi, and M.-S. Alouini, "Channel modelling and performance analysis of V2I communication systems in blind bend scattering environments," *Progress In Electromagnetics Research B*, vol. 57, pp. 233–251, 2014.

[7] R. Khedhiri, N. Hajri, N. Youssef, and M. Patzold, "On the first-and second-order statistics of selective combining over double Nakagami-m fading channels," in *IEEE Vehicular Technology Conference*, 2014.

[8] A. Chandra, C. Bose, and M. K. Bose, "Unified BER and optimum threshold analysis of binary modulations in simple and cascaded Rayleigh fading channels with switched combining," *International Journal of Communication Systems*, vol. 24, no. 2, pp. 153–167, 2011.

[9] J. Reig, L. Rubio, and N. Cardona, "Bivariate Nakagami-m distribution with arbitrary fading parameters," *Electronics Letters*, vol. 38, no. 25, pp. 1715–1717, 2002.

[10] N. C. Sagias and G. K. Karagiannidis, "Gaussian class multivariate Weibull distributions: theory and applications in fading channels," *IEEE Trans. Inf. Theory*, vol. 51, no. 10, pp. 3608–3619, Oct. 2005.

[11] M. K. Simon and M.-S. Alouini, *Digital Communication over Fading Channels*, 2nd ed. New York: Wiley, 2005.

[12] I. S. Gradshteyn and I. M. Ryzhik, *Table of Integrals, Series, and Products*, 6th ed. New York: Academic Press, 2000.

[13] A. Prudnikov, Y. Brychkov, and O. Marichev, *Integrals and Series, Volume 1*. Gordon and Breach Science Publishers, 1986.

[14] The Wolfram Functions Site, 2015. [Online]. Available: http://functions.wolfram.com

[15] Y. Chen and C. Tellambura, "Distribution function of selection combiner output in equally correlated Rayleigh, Rician, and Nakagami-m fading channels," *IEEE Trans. Commun.*, vol. 52, no. 11, pp. 1948 – 1956, Nov. 2004.

[16] G. K. Karagiannidis, D. A. Zogas, and S. A. Kotsopoulos, "On the multivariate Nakagami-m distribution with exponential correlation," *IEEE Trans. Commun.*, vol. 51, no. 8, pp. 1240–1244, Aug. 2003.

[17] P. Kyosti, 2007. [Online]. Available: WINNER II Channel Models, DR1.1.2. https://www.ist-winner.org/WINNER2-Deliverables/D1.1.2v1.1.pdf

[18] V. S. Adamchik and O. I. Marichev, "The algorithm for calculating integrals of hypergeometric type functions and its realization in REDUCE system," in *International Conference on Symbolic and Algebraic Computation*, Tokyo, Japan, 1990, pp. 212–224.